Process Safety and Environmental Protection

Rok 2021, Volume 156

December

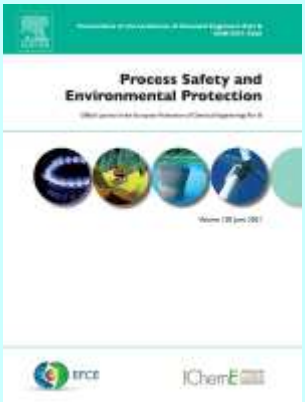

Xueqiang Shi, Xiaokun Chen, Yutao Zhang, Yuanbo Zhang, Zhicheng Shi, Bo Che, Shangwen Xia. Characteristics of self-ignition and smoldering of coal dust layer under inclination conditions. Pages 1-16.

In many actual industrial scenes, the coal body and coal dust are not always in the tiled state, but in the inclined situation. A two – dimensional transient numerical model of coal oxidation reaction was established to study the self-ignition and smoldering characteristics of coal dust layers in the presence of inclination angle. The effects of gravity and thermal buoyancy were considered to solve the coupling problem of coal oxidation reaction and air flow. The results show that the growth coefficients of minimum ignition temperature of coal dust with thicknesses of 6.4 mm, 12.7 mm, 19.1 mm and 25.4 mm are 0.117 °C/°, 0.0467 °C/°, 0.033 °C/° and 0.033 °C/°, respectively. With the increase of hot plate temperature, the inclination of coal dust can greatly shorten the ignition delay time (IDT). The ΔIDT of coal dust inclination of 60° is 128 s/°C greater than that of 0°. The movement of high temperature point of coal dust in self-heating development stage is from the inside to the outside, and that in decaying stage is from the outside to the inside. In addition, some interesting phenomena in the process of coal self-ignition and smoldering have also been found. The influence of coal dust inclination on its self-heating is mainly reflected in the location of high temperature points and the spread of smoldering. This study is helpful to understand the characteristics of coal dust self-ignition and smoldering spread in inclined situation, and can guide the prevention of coal dust self-ignition.

- **Keywords:** Coal dust; Numerical simulation; Self-ignition; Inclination angles; Smoldering

Xuyan Liu, Hong Yang, Shaolun Wang, Xiaoyue Fang, Xiaotong Wang, Yongsheng Bai, Bojun Su, Luyuan Shi. *Study on the effectiveness of an independent biological phosphorus removal system based on immobilized biological fillers nitrogen removal system in municipal wastewater*. Pages 17-28.

This study focused on the problem that simultaneous nitrogen and phosphorus removal cannot be achieved in current urban sewage treatment systems. To address this, a pilot system was developed to first use immobilized biologically active fillers to remove nitrogen, and then use activated sludge to independently remove phosphorus. The goal was to maximize the effectiveness of biological phosphorus removal. This study mainly aimed at analyzing the post-independent phosphorus removal characteristics and mechanisms; the composition of the phosphorus removing bacteria; and the contribution rate of the system. The effluent PO43--P of the system remained stable at 0.15–0.2 mgL−1, with the phosphorus removal anaerobic tank maintaining a "micro-release" state. When the hydraulic retention time (HRT) of the aerobic phosphorus removal tank was reduced to 1 h, the contribution rate of the aerobic phosphorus removal bacteria decreased from 28.42% to 16.68%; the contribution rate of the denitrifying phosphorus removal bacteria increased from 72.58% to 83.32%; and the abundance of the dominant bacteria Dechloromonas and Thaurea significantly increased. The phosphorus removal system provides a new approach for deep phosphorus removal in main municipal wastewater systems.

- **Keywords:** Immobilized filler; Post-independent biological phosphorus removal; Micro-release state; Phosphorus removal contribution; Microbial community structure

Jinchun Zhang, Xin Chen, Jinxiu Hou, Wenjun Zhang, Shilong Wu. *Early risk warning method for fluidized beds using generalized extremum distribution of pressure fluctuation*. Pages 29-42.

Pressure fluctuation is commonly used to characterize the dynamic of fluidized bed, and bubble movements resulting in pressure fluctuations will seriously affect the stable operation of fluidized bed. This paper presents an extreme value statistical analysis model that uses generalized extreme value (GEV) distribution to analyze the pressure fluctuation time series, predict its future fluctuation state, and further provide risk warning for fluidized bed operation. The pressure fluctuation time-series for four mainly fluidization behaviors (single bubble, multiple bubble, exploding bubble and transport conditions) in an actual experiment were analyzed by the proposed method. The results show that the error rate of the proposed method in this paper is controlled within±10%, and the average error rate is controlled within −1.7%–3.7%. By analyzing the risk margin of the extreme pressure fluctuations of each flow regime, the risk margin of exploding bubble is the largest, and more stringent measures should be taken to ensure the stable operation of the fluidized bed in this flow state. In summary, the risk warning of the fluidized bed can be detected in the joint efforts of the confidence interval and the risk margin of the pressure fluctuation return level of each flow regime.

- **Keywords:** Fluidized bed; Pressure fluctuation; Generalized extreme value distribution; Risk margin; Risk early warning

D.O. Glushkov, G.S. Nyashina, R. Anand, P.A. Strizhak. *Composition of gas produced from the direct combustion and pyrolysis of biomass*. Pages 43-56.

Biomass is considered to be one of the most easily available and high-potential renewable power sources. Pyrolysis and combustion are the most common ways of utilizing biomass. A complex multiple-criteria analysis to identify the most promising technology of using various types of biomass has never been previously performed. The study is focused on comparing two typical techniques of utilizing agricultural and forestry biomass for bioenergy and valorization. In this paper, the direct combustion and pyrolysis of biomass were experimentally studied. The environmental and energy performance parameter of the investigated processes were determined for separate biomass components (leaves, straw, sawdust) and a group of mixtures from them. It was

established that the biomass mixtures combustion has better environmental characteristics. Thus, the main anthropogenic emissions decreased by 8–66%. In addition to that, the pyrolysis of a biomass mixture from a group of components has a 30% higher yield of combustible gases. The analysis of relative efficiency indicators of two processes where biomass was used as an energy resource showed that a biomass-derived composite fuel is more efficient than its individual components.

- **Keywords:** Biomass; Pyrolysis; Combustion; Power generation; Environment; Efficiency

Yansheng Wang, Cunbao Deng, Zhixin Jin, Qian Liu, Ling Qiao. *Definition and mathematical expression on instability domain of safety event and safety structure*. Pages 57-71.

Dynamic risk assessment is a main research task of process safety. One of the main methods of dynamic risk assessment is to measure the distance between the real-time state and its threshold (dangerous state). Due to the influence of temperature, pressure and other factors, the dangerous state will often be expanded into a "dangerous range" of states. At present, most of the "dangerous range" are determined subjectively or according to experiences. Based on the safety structure theory, instability domain as the scientific term of "dangerous range" is proposed, and then its mathematical expression is developed in this paper. The safety structure composed of an atomic activity factor (AAF) and an atomic environmental factor (AEF) is regarded as the smallest unit to analyze safety issues in safety structure theory. When the state of a safety structure falls into its instability domain, the state of intrinsic factor will fall into the instability domain of the safety event. This is a sufficient condition to cause an accident. In this paper, the attribute of intrinsic factor about a safety event is determined by developing the performance extension membership function of the intrinsic factor, thus the mathematical expression on instability domain of the safety event is established. Taking the instability domain of safety event as the domain of the inverse mapping of state relationship functions among environmental factors, and then the mathematical expression on atomic environmental instability domain (AEID) of safety structure is established. Taking AEID as domain of the inverse mapping of state relationship function between AAF and AEF, thus the mathematical expression on atomic activity instability domain (AAID) of safety structure is established. The instability domain of safety structure is composed of AEID and AAID together. The mathematical expression on instability domains can provide theoretical basis for the dynamic risk assessment, prediction and active control of safety accidents.

- **Keywords:** Process safety; Accident; Dynamic risk assessment; Critical value; Instability domain; Safety structure

Kai Yang, Yanbin Chen, Qiuping Xiao, Lei Pang. *Influence of venting coefficient on disastrous effects of aluminium powder explosions*. Pages 72-88.

Aluminium powder has a very high risk of explosion. To clarify the disastrous effects of the overpressure and high temperatures during an aluminium powder explosion in a constrained space and the distribution of the outdoor safe distance, the explosion and venting processes of aluminium dust in a large-scale building were investigated under different venting coefficients, Kv (Kv = Av/Ap), using computational fluid dynamics (CFD). The results show that although an increase in the venting coefficient can reduce the indoor overpressure and explosion temperature, it can also increase the distance up to which the outdoor overpressure and high temperature can cause damage. Moreover, the distance up to which explosion overpressures can be harmful to personnel and buildings increases with an increase in the venting coefficient. Hence, the safe outdoor distance may be more than 1.5–2 times the fire safe distance listed in the Chinese Code

for fire protection design of buildings. The high-temperature damage caused by the explosion also increases with an increase in the venting coefficient. Therefore, the current explosion safety protection distances for aluminium powder production sites need to be revised.

- **Keywords:** Aluminium powder; Explosion venting; Vent size; High temperature; Overpressure; Safe distance

Shengshu Ai, Linzhu Du, Zebing Nie, Ziheng Wang, Chunlin Chang, Wenai Liu, Fan Wang, Dejun Bian. Study on nitrogen removal mechanism of the micro-pressure double-cycle reactor. Pages 89-99.

To explore the reasons for the excellent denitrification performance of the Micro-pressure double-cycle reactor (MPDR), the nitrogen removal mechanism of the reactor in the treatment of municipal wastewater was studied. Through analysis of flow simulation and dissolved oxygen (DO) distribution, it was determined that the reactor had a macroscopic biochemical reaction environment for simultaneous nitrification and denitrification (SND) because of the special structure of reactor. The result of sewage treatment showed that the average removal rates of COD, NH4+-N, TN, TP were 92.29%, 96.64%, 73.6% and 91.66% respectively, and the SND rate was 60.9%. Dechloromonas, Thermomonas, Micropruina, Tetrasphaera, etc. for nitrogen and phosphorus removal existed in the reactor at the same time to explain the excellent performance of the system. PICRUSt2 showed that the metabolic pathways related to nutrient degradation in the reactor were highly active and the abundance of denitrification functional genes was higher in the central zone and lower in the peripheral zone. The research results not only perfected the basic theory of the reactor, but more importantly, provided theoretical and technical support for the further application of the reactor.

- **Keywords:** Distribution of dissolved oxygen; Functional zones; Micro-pressure double-cycle reactor; Nitrogen removal; PICRUSt2; Simultaneous nitrification and denitrification

Erjun Zhang, Kanggen Zhou, Xuekai Zhang, Yehuizi Wu, Jiajian Liu, Wei Chen, Changhong Peng. *Selective separation of copper and zinc from high acid leaching solution of copper dust using a sulfide precipitation-pickling approach*. Pages 100-108.

Herein, a new approach for direct separation of Cu and Zn from high acid leaching solution was proposed. The approach includes two steps, Cu and part of Zn first precipitated with H2S, then the Zn in the residue was re-leached using the original leaching solution. Thermodynamics calculation indicates that CuS and As2S3 will generate even the acid concentration is over 8 mol/L, while ZnS is easier to dissolve in acid solution. Therefore, it is possible to selective separate Cu and Zn using H2S under high acid concentration. Key parameters which will affecting the precipitation of Cu and the pickling of Zn are systematically investigated. Under the optimal conditions, the precipitation efficiency of Cu can reach over 99%, and the loss of Zn was only 3.15%. Moreover, more than 96% of As in the leaching solution will also be precipitated. The concentrations of Cu, As, and Zn in the leachate are 0.0722, 0.0893, 48.73 g/L, respectively. The content of Cu in the residue can reach over 57% which could be used for extraction of Cu. XRD results showed that Cu and As were existed as CuS and As2S3 in the residue.

- **Keywords:** Cu precipitation; Separation; High acid leaching solution; H2S; Pickling

Esther Vega, Héctor Valdés. *Regeneration of odorous sulphur compound-exhausted activated carbons using wet peroxide oxidation: The impact of chemical surface characteristics*. Pages 109-120.

The efficiency of hydrogen peroxide in the regeneration of dimethyl sulphide (DMS) exhausted-activated carbons (ACs) is assessed in this study. Moreover, the influence of chemical surface composition is evaluated using six ACs (two commercial ACs and four chemically modified ACs) with different surface features. Chemical surface composition of ACs before and after different adsorption-regeneration cycles is assessed by temperature-programmed desorption coupled with mass spectroscopy (TPD-MS) and by diffuse reflectance infrared Fourier transform spectroscopy (DRIFTS). Results reveal that up to a 60% of regeneration efficiency is attained, being more effective in the presence of ACs derived from Filtrasorb 300 AC sample. Experimental findings show that ACs with high content of basic oxygen–containing functional surface groups and mineral fraction are responsible to promote the catalytic decomposition of hydroxide peroxide, leading to a higher formation of hydroxyl radicals and to the observed increase in the regenerative oxidation of adsorbed DMS. However, a decrease in removal efficiency is related to an increase in the amounts of oxygen functionalities mainly in the form of strong acidic surface groups such as carboxylic acid anhydrides and carboxylic acids that shift the reaction mechanism from promoting the initiation of radical chain reactions to termination. Additionally, DRIFTS analyses indicate that after successive adsorption-regeneration cycles the fraction of organic molecules that remains adsorbed limits the access to active surface sites responsible for radical generation, reducing drastically the catalytic activity of ACs.

- **Keywords:** Activated carbon; Dimethyl sulphide; Hydrogen peroxide; Regeneration; Sulphur compounds

Ziyan Ren, Wei Zeng, Hongjun Liu, Yuan Jia, Xiaojing Peng, Yongzhen Peng. *Enhanced bioavailability of phosphorus in sewage sludge through pyrolysis aided by calcined clam shell powder*. Pages 121-133.

Phosphorus is an indispensable element, while the existing phosphate rock resources are not enough to maintain the long-term demand of modern agricultural development. To ensure the sustainability of economic and social, it is necessary and urgent to seek the alternative phosphorus source of phosphate rock. In this study, calcined clam shell powder (CSP) was firstly used as a modifier and mixed with sewage sludge (SS) for co-pyrolysis to obtain sludge-derived pyrochars containing a large amount of bioavailable phosphorus. The effect of different temperatures (500, 600, 700, 800 °C) and dosages (0%, 10%, 20%, 30%) on the change in the form of phosphorus during the pyrolysis process were investigated. With the increase of temperature and the addition of CSP, the orthophosphate (Ortho-P) increased from 63.69% in the original SS to nearly 100%. Furthermore, the main phase of inorganic phosphorus (IP) changed, mainly in the form of apatite phosphorus (hydroxyapatite increased from 8.88% to 35.97%), and the concentration of easy-to-lose phosphorus reduced to 0.11 mg/g. After co-pyrolysis of SS with CSP, the passivation situation of heavy metals (HMs), such as Zn, Mn, Cr, Cu, Cd and Pb was significantly improved, thus reducing the potential environmental risk. The planting experiment proved that the sludge-derived pyrochars obtained by adding 20% CSP at 800 °C promoted the germination of seeds and the growth of seedlings. Consequently, the product of SS co-pyrolysis with CSP could be used as an excellently bioavailable and environmentally friendly phosphate fertilizer for agricultural production.

- **Keywords:** Sewage sludge; Calcined clam shells; Co-pyrolysis; Heavy metals; Phosphorus bioavailability

Diego Alberto Morales Urrea, Analía Verónica Fernández Gimenez, Yamila Eliana Rodriguez, Edgardo Martín Contreras. *Immobilization of horseradish peroxidase in Ca-alginate beads: Evaluation of the enzyme leakage on the overall removal of an azo-dye and mathematical modeling*. Pages 134-143.

Horseradish peroxidase (HRP) was immobilized in calcium alginate beads by extruding an alginate/HRP solution through a syringe onto calcium chloride. The aim of this study was to evaluate their use to remove the azo-dye Orange II (OII), under different experimental conditions, such as the number of beads, pH, reuse of the biocatalyst, hydrogen peroxide feeding strategy. A mathematical model that takes into account the diffusion of reactants, products, and HRP throughout the beads and the effect of the enzyme leakage on the observable oxidation rate was also developed. Results indicated that the immobilization efficiency decreased as a function of the incubation time in CaCl2. Although enzyme-containing beads had a low OII adsorption capacity, under the presence of hydrogen peroxide, the dye removal was highly increased due to the catalytic activity of HRP. Besides, the initial OII oxidation rate (RS0) using 3 beads at pH 9 was higher than at pH 7. Also, RS0 increased as a function of the number of tested beads. The developed model was fitted to experimental data obtained at different conditions. Then, the model was validated against a new data set that was not used for the calibration of the model, obtaining a satisfactory agreement between simulation results and these new data. Simulations demonstrate that 70–90% of the total OII removed was due to its oxidation by hydrogen peroxide catalyzed by HRP in the liquid phase.

- **Keywords:** Horseradish peroxidase; Hydrogen peroxide; Ca-alginate beads; Enzyme leakage; Modeling

Yinggui Xu, Jinlong Li, Qing Ye, Yudong Li. *Energy efficient extractive distillation process assisted with heat pump and heat integration to separate acetonitrile/1,4-dioxane/water*. Pages 144-159.

Two energy efficient extractive distillation processes are proposed to separate acetonitrile/1,4-dioxane/water mixture in this study. The COSMO-SAC model is chosen to screen suitable entrainer and dimethyl sulfoxide is selected. Process intensification technologies of heat pumps and heat integration are utilized in the processes for energy conservation. Several evaluation methods containing energy, economic, environmental and exergetic analysis are introduced to evaluate the performance of different processes. The most energy-saving and environmental friendly process is heat pump assisted direct extractive distillation that achieves an energy reduction by 53.58% and a carbon dioxide emission reduction by 53.56% compared to the indirect scheme, while the direct scheme assisted with heat integration performs best that achieves a reduction by 40.38% on total annual cost.

- **Keywords:** Separation; Extractive distillation; Heat integration; Heat pump

Bahram Ghorbani, Armin Ebrahimi, Mostafa Moradi. *Exergy, pinch, and reliability analyses of an innovative hybrid system consisting of solar flat plate collectors, Rankine/CO2/Kalina power cycles, and multi-effect desalination system*. Pages 160-183.

Nowadays due to increasing energy demand in the world, the use of energy systems with maximum efficiency is unavoidable. Thermal integration of the systems decreases the number of equipment employed and also raises the efficiency of the hybrid configuration. In the present study, an innovative hybrid system for cogeneration of power and desalinated water including organic Rankine unit, carbon dioxide power plant, Kalina

power cycle based on the seawater temperature difference, and multi-effect desalination system is developed. Part of the heat required by the system is provided by solar flat plate collectors. The innovative hybrid system produces 849.5 MW power and 198.5 kg/s potable water. Exergy investigation of the system indicates that the most exergy destruction in the whole system belongs to the combustion chamber and heat exchangers, each of which is 46.60% and 34.91% of the total exergy destruction, respectively, which shows that more than 80% of exergy destruction is related to these two parts. The exergy efficiency of the whole system is 44.81%. Through the pinch method, the heat exchanger network related to the multi-stream heat exchangers of the hybrid system is extracted. The effect of air /fuel ratio (inlet to the combustion chamber) on system performance in the parametric analysis is examined. One of the main results is a 12.69% improvement compared to the initial state of total electrical efficiency of the structure in case of increasing the fuel input to the combustion chamber up to 62.00 kg/s. By system reliability analysis and examining different modes of failure and repair rates of different sections of the system, the probability of the structure operation in different cases is extracted.

- **Keywords:** Integrated power generation; Rankine/CO2/Kalina power cycles; Solar flat plate collectors; Multi-effect desalination; Pinch and exergy analyses; Reliability assessment

Carlos Magno Tolentino Filho, Heloísa Bremm Madalosso, Carolina D' Ávila Kramer Cavalcanti, Miguel Angelo Granato, Ricardo Antonio Francisco Machado, Cintia Marangoni. *Influence of multi-component composition of dyeing bath in the membrane distillation performance*. Pages 184-195.

The influence of the multi-component composition of cotton and polyester dyeing baths was investigated in a DCMD process using a PTFE membrane, aiming to water reclamation from textile wastewater. The process was evaluated with each auxiliary, solutions combining auxiliary and dye, and residual water from pilot-scale dyeing baths. The salts used in the cotton dyeing bath did not influence the DCMD process, resulting in a similar rejection rate and permeate flux to those in dye solutions. The formic acid employed in the polyester dyeing bath resulted in high permeate fluxes but decreased the permeate quality by almost 33%. The surfactants (detergent and dispersant) demonstrated the most harmful behavior in the process, evidenced by a complete membrane wetting. An absence of synergy of the dyes and auxiliaries influencing the DCMD process was verified for the textile dyeing wastewater. This work enabled identifying the influence of each dyeing bath component in the rejection rate and permeate flux, allowing to find alternatives in mitigating the remaining gaps involving DCMD operation and the MD membranes. This work contributes to consolidating this promising technique in water reclamation from textile wastewater, encouraging research on membrane development and modification or integrated operations involving MD.

- **Keywords:** Auxiliary; Cotton; DCMD; Polyester; Textile wastewater; Water recuperation

Kuibin Zhou, Xuan Nie, Chao Wang, Yandong Wang, Huichang Niu. *Jet fires involving releases of gas and solid particle*. Pages 196-208.

The high-pressure leakage of underground pipeline could entrain the nearby sands and soils, and thus cause the jet fire of gas-solid mixtures. In addition, the thermal runaway of Lithium ion batteries could also cause a typical gas-solid jet diffusion flame. In comparison with the gaseous jet diffusion flame and the gas-solid-air jet premixed flame, the gas-solid jet diffusion flame lacks of exploration. Thus, a new facility consisting of a jet fire apparatus and a sand feeder, was designed to explore the gas-solid jet fire. The

test repeatability was justified for the proposed facility. The dynamical differences of gas-solid and gaseous jet fires are clarified. It is found that the gas-solid jet fire holds a larger lift-off height, a less visible flame height and a less radiative fraction than the purely gaseous jet fire. In particular, for gas-solid jet fires at high exit velocities, the lift-off height increases, but the visible flame height and radiative fraction seem to decrease, as the particle size of sand decreases to increase the jet height of sand. (1) Inside the flame volume, the sand plays a role of heat sink to decrease the flame temperature and thus the flame burning velocity. Moreover, in the lift-off region, the sand dilutes the gas fuel and isolates the surrounding oxygen to inhibit the combustion. Both effects of sand cause a large lift-off height, especially for the sand of little particle size. (2) A large lift-off height means the increase of the air mass entrained from flame base or the portion of the premixed flame to the whole flame. In addition, the sand particle-laden flow would significantly increase the ambient air entrainment rate of fire plume. Both effects result in a less visible flame height. (3) The portion of the premixed flame increases in the bottom, which reduces the total soot amount inside the whole flame volume. The decrease of the flame temperature and the total soot amount reduces the radiative fraction. (4) The sand significantly affects the flame geometry and radiative fraction, which alters the radiant heat flux distribution and challenges the development of thermal radiation model for gas-solid jet fires. The gas-solid jet fire holds a less peak radiant heat flux but a higher positon of peak radiant heat flux than the gaseous jet fire. In addition, the line source radiation model available in literature is revised to well predict the radiant heat flux distribution of the gas-solid jet fires.

- **Keywords:** Jet flame; Gas-solid mixture; Lift-off height; Flame height; Radiative fraction; Radiation model

Rui Zhang, Zongyuan Zhu. *Microwave assisted hydrothermal conversion of waste cardboard*. Pages 209-218.

The conversion of waste cardboard using microwave assisted hydrothermal method to obtain reducing sugars and versatile chemical blocks is reported in this work. The findings revealed that microwave assisted dilute acid hydrothermal conversion of cardboard is effective and efficient, as it removed considerable amount of CaCO3 in cardboard to keep the microwave conversion pressure at a stable status and can selectively produce value-added chemicals by changing the conversion temperature. The optimum conversion conditions for maximum aqueous bio-oil yield (29.76 wt%) was using 0.1 g of cardboard and 10 g of 2.5 wt% of phosphoric acid at MW hydrothermal condition of 175 °C for 30 min. Products compositions were changed and refined by changing the dilute acid MW hydrothermal conditions. At 150 °C, sugars were the main products; at 175 °C, levoglucosan was the main product whereas at 200 °C the major product was levulinic acid.

- **Keywords:** Waste management; Cardboard; Microwave assisted conversion; Reducing sugars; Levulinic acid

Rose Fadzilah Abdullah, Umer Rashid, Mohd Lokman Ibrahim, Muhammad Amirrul Hakim Lokman NolHakim, Bryan R. Moser, Fahad A. Alharthi. *Bifunctional biomass-based catalyst for biodiesel production via hydrothermal carbonization (HTC) pretreatment – Synthesis, characterization and optimization*. Pages 219-230.

The hydrothermal carbonization (HTC) technique is known for its advantages in producing hydrochar from biomass samples with high water content compared to conventional pyrolysis techniques. This study utilized HTC to produce an activated carbon catalyst from renewable mesocarp fiber derived from palm oil processing. The introduction of K2CO3 and Cu(NO3)2 produced a bifunctional catalyst suitable for

conversion of used cooking oil to biodiesel. The catalyst possessed a mesoporous structure with a BET surface area of 3909.33 m2/g. An optimum treatment ratio of 4:1 (K2CO3: Cu(NO3)2) provided elevated basic (5.52 mmol/g) and acidic (1.68 mmol/g) concentrations on the catalytic surface, which promoted esterification and transesterification reactions. Maximum yield (96.4%) of biodiesel was obtained at 70 °C for 2 h with 5 wt% catalyst and a 12:1 molar ratio of methanol to oil. The catalyst endured up to 5 reaction cycles while maintaining biodiesel yields of more than 80%. These findings indicated that HTC pretreatment yielded a high-quality bifunctional catalyst for conversion of low-quality used cooking oil for production of biodiesel.

- **Keywords:** Hydrothermal carbonization; Biomass-based activated carbon; Bifunctional catalyst; Biodiesel; Fatty acid methyl esters; Transesterification; Esterification

Yunhao Li, Juncheng Jiang, Yuan Yu, Zhirong Wang, Zhixiang Xing, Qingwu Zhang. *Fire resistance of a vertical oil tank exposed to pool-fire heat radiation after high-velocity projectile impact*. Pages 231-243.

Due to the complex effects of combined loadings on complete steel structures, the combined effects of high-velocity projectile impact and heat radiation due to a pool-fire on a vertical Q345 steel tank have not been generally considered. In this study, a consecutive coupling approach is established. The combined effects of projectile perforation and heat radiation on the failure modes and fire resistance of a vertical steel tank are investigated. Additionally, the effects of the projectile size, projectile shape, and separation distance are analyzed. The results indicate that compared with a fixed-roof tank without impact, the perforation results in stress concentrations in the plastic deformation zone. The stress level of the perforated tank is higher, and the fire resistance of the perforated tank is lower. Additionally, as the perforation size increases, the stress level triggering the thermal buckling of the perforated tank decreases outside of the plastic deformation zone. Additionally, the fire resistance decreases. Moreover, as the separation distance decreases, the stress level of the cylindrical shell increases. The fire resistance of the perforated tank decreases dramatically. By understanding the failure mode, this study is able to suggest fire and explosion protection measures in petrochemical industries to decrease or eliminate the domino effect risk and incident damage. Additionally, the fire resistance data can help improve guidelines and understanding for fire and rescue services, which would undoubtedly play a vital part in emergency response and rescue, and enhance the process safety level overall.

- **Keywords:** Combined loadings; Heat radiation; Projectile perforation; Failure modes; Fire resistance; Vertical steel tank

Yunhao Xi, Tianqi Liao, Jing Li, Libo Zhang. *Mechanism of zero-valent lead reduction for removing high concentration of arsenic from waste acid of lead smelting system*. Pages 244-255.

Lead metal smelting waste acid containing high concentrations of arsenic and sulfuric acid threaten human health and pose huge potential environmental risks due to its possible leakages during storage and disposal. In order to remove arsenic in smelting waste acid, a new method for arsenic removal by adding zero-valent lead and CuSO4 is proposed. The substitution reaction between zero-valent lead and CuSO4 to generate Cu0, and form a Pb-Cu galvanic cell system with zero-valent lead. Through the reduction of zero-valent lead, As(III) was reduced to As(0) and reacted with Cu0 to produce Cu3As precipitation. As the pH of waste acid changed, AsO2- will produce As2O3. When the molar ratio of Pb to As (Pb/As) was 6, CuSO4 concentration was 7 g/L, 25 °C, and 240 min, the arsenic concentration sharp decreased from 4706.4 mg/L to 35.21 mg/L, arsenic removal efficiency reached 99.25%. The arsenic removal process could be described by the shrinking core model which was controlled by a diffusion process. XRD,

SEM-EDS, and XPS were used to characterize the phase, morphology, and elemental valence of the arsenic-containing precipitates. Based on the above analysis and combined with thermodynamic analysis, the mechanism of arsenic removal by zero-valent lead combined with CuSO4 was revealed.

- **Keywords:** Arsenic; Waste acid; Zero-valent lead; Reduction reaction; Kinetics

Ayushman Bhattacharya, Ambika Selvaraj. *Photocatalytic conversion of CO2 into beneficial fuels and chemicals – a new horizon in atmospheric CO2 mitigation*. Pages 256-287.

Global industrialization and overreliance on fossil fuels for energy has triggered higher atmospheric CO2 concentrations and resulted in global warming. This fact necessitates the elimination of CO2 in the atmosphere. Inspired by natural photosynthesis and driven by the advancement in nanotechnology, the application of 2D-semiconductors in the photocatalytic conversion of CO2 into beneficial products such as C1 and C2 compounds has gained significant momentum in research worldwide. Having understood the importance of this research area, this review discusses the fundamentals and in-depth mechanism of photocatalytic reduction of CO2 in synergy with various reaction pathways. Besides, it recapitulates the emerging and recently developed highly efficient, selective, and active photocatalysts for CO2 conversion. Also, the study incorporates the critical performance assessment of the various photocatalysts in the different reaction mediums and details various modification strategies with dopants, functional groups, co-catalyst, surface defects, and heterojunction band bending along with their roles in the enhancement of photocatalytic reduction of CO2. This review article is the first of its kind in covering the aspects of chemistry in the material - environment - energy nexus. Hence, it will be useful for the researchers and applicants working in the field of environmental engineering, materials science, energy, chemistry, and chemical engineering.

- **Keywords:** Photocatalytic CO2 reduction; Recombination; Band bending; Heterojunction; Doping; Vacancy engineering; Functional groups

Cheng Sun, Liang Guo, Yongkang Zheng, Dan Yu, Chunji Jin, Yangguo Zhao, Zhiwen Yao, Mengchun Gao, Zonglian She. *The hydrolysis and reduction of mixing primary sludge and secondary sludge with thermophilic bacteria pretreatment*. Pages 288-294.

Hydrolysis is widely used in sludge treatment as it enables to improve the biodegradability of sludge. However, there was little information about the hydrolysis efficiency with the mixture of primary and secondary sludge. In this study, the hydrolysis and reduction of mixed sludge after thermophilic bacteria (TB) pretreatment was investigated. Volume ratio of 1:3 (primary sludge: secondary sludge) had best release rate of organics, and the soluble chemical oxygen demand (SCOD), carbohydrate and protein in extracellular polymeric substances (EPS) decreased by 7.9, 4.1, 7.2 times, respectively. Meanwhile, the accumulation of SCOD, carbohydrate and protein in dissolved organic matter (DOM) was enhanced with mixed sludge. Excitation-emission matrix (EEM) spectroscopy proved that mixture of sludge was beneficial for the releasing of biodegradable substances. The sludge reduction of mixed sludge was higher than that of single sludge, and mixed sludge (1:3) had the best suspended solid (SS) and volatile suspended solids (VSS) reduction rate of 27.2% and 34.3%.

- **Keywords:** Primary sludge; Secondary sludge; Mixed sludge; Hydrolysis; Thermophilic bacteria (TB)

Houli Li, Jin Hu, Yixiao Wang, Xuebin An, Mingzhu Tang, Zhiying Wang, Yunshan Wang, Gang Yang, Weijun Bao, Yong Sun. *Utilization of phosphogypsum waste through a temperature swing recyclable acid process and its application for transesterification*. Pages 295-303.

In this paper, a biodiesel catalyst was prepared from the phosphogypsum (PG) by a hybrid approach through temperature swing acid leaching/crystallization steps followed by the subsequent fluidized bed calcination. The impacts of acid leaching and crystallization were extensively analyzed via a supervised machine learning approach using a limited number of experimental runs to find out the optimal condition. The determined optimal conditions are X1-95 (ºC), X2-30 (min), X3-30 (wt%-H2SO4), and corresponding validation experimental result (at the optimal condition setting) shows± 5% uncertainties. The prepared catalyst predominately contains CaSO4 (98 wt%) with the impurities less than 0.3 wt% (i.e., P2O5- and F-). The numbers of acid leaching cycles (up to 10 cycles) were investigated, and result indicates a good contaminates recovery (P2O5:1.8 g/100 g PG, Mg2+: 0.3 g/100 g PG, Al3+: 0.3 g/100 g PG, Fe3+: 0.1 g/100 g PG) in the leachate through the downstream solvent extraction. The catalytic conversion reaches about 50% with approximately± 5% deactivation when catalyst was reused at the same transesterification condition. The decreased binding energies of S2p (169.6 eV) and O1st (533 eV) in used catalyst indicate the deactivation of surface catalytic sites. The key properties of the prepared biodiesel are comparable to the American society for testing and materials (ASTM) standards.

- **Keywords:** Phosphogypsum; Biodiesel; Catalyst; Machine learning optimization

Mahdi Elyasi Kojabad, AliAkbar Babaluo, Akram Tavakoli, Haniyeh Golizadeh Kahnamouei. *A novel high-performance facilitated transport membrane by simultaneously using semi-mobile and fixed carriers for CO2/N2 separation*. Pages 304-314.

In this study, poly (ether-block-amide) (Pebax) facilitated transport membranes (FTMs) containing aniline, and ionic liquid (IL) modified alumina (M-Al) particles were prepared. Aniline molecules acted as semi-mobile carriers and IL-modified particles as fixed carriers for CO2 molecules in these membranes. Different amounts of M-Al particles were added to the Pebax/aniline (50 wt%) membrane, and a facilitated transport membrane containing 5 wt% M-Al particles was obtained as the optimal membrane. For Pebax/aniline (50 wt%)/M-Al (5 wt%) membrane, CO2 permeability was 167 barrer, and CO2/N2 selectivity was 123 increased by 94% and 168% compared to pure Pebax membrane, respectively. The CO2 separation performance of the prepared FTMs was also evaluated in the humidified state. The results showed that in the presence of water, the amino groups in the structure of aniline and IL performed better and improved the facilitated transport mechanism. Therefore, for all FTMs, CO2 permeability significantly increased in the humidified state so that CO2 permeability and CO2/N2 selectivity reached 406 barrer and 123, respectively, for optimal membrane. The molecular simulation was used to study details of the motion of aniline molecules in the polymeric matrix. The simulation and experimental results confirmed each other and showed that the presence of aniline prevents the hopping mechanism from stopping even at low concentrations of particles as fixed carriers and creates a combined hopping-vehicle mechanism in the membrane structure that results in excellent performance membranes.

- **Keywords:** Ionic liquid; Facilitated transport membrane; Molecular simulation; CO2 separation

Bamidele Victor Ayodele, May Ali Alsaffar, Siti Indati Mustapa, Adesoji Adesina, Ramesh Kanthasamy, Thongthai Witoon, Sureena Abdullah. *Process intensification of hydrogen production by catalytic steam*

***methane reforming: Performance analysis of multilayer perceptron-artificial neural networks and nonlinear response surface techniques*. Pages 315-329.**

Uncertainty about how process factors affect output might lead to waste of resources in laboratory experiments. To address this constraint, a data-driven method might be used to describe the non-linear connection between process parameters and desired output. A Multi-Layer Perceptron-Artificial Neural Network (MLP-ANN) and non-linear response surface method are used to predict hydrogen generation by catalytic steam methane reforming. The impact of training methods (scaled conjugate and gradient descent), hidden layer variation, artificial neuron variation, and activation functions were studied in 80 MLP-ANN combinations (hyperbolic tangent function and sigmoid function). The performance of MLP-ANN models was affected by the training techniques, activation functions, layer count, and number of artificial neurons. The model with the sigmoid function and 3 input layers, 17 artificial neurons in the first layer, 15 artificial neurons in the second layer, and 2 output nodes had the greatest performance among the 40 configurations of scaled conjugate trained ANNs. It projected an 89.55% maximal hydrogen yield with a coefficient of determination (R2) of 0.997 and reduced errors with Mean absolute percentage error (MAPE) and mean squared error (MSE) of 0.199 and 0.121, respectively. Similarly, the gradient descent ANN model with hyperbolic tangent activation function had the greatest performance among the 40 gradient descent trained-ANN configurations. The 3–15–7–2 gradient descent trained ANN model projected a maximum hydrogen output of 89.73% compared to the experimental results of 89.51%. The MLP-ANN models outperformed nonlinear response surface methods, with R2, MAPE, and MSE of 0.231, 0.191, and 0.988, respectively. The updated Garson algorithm indicated that the input parameters impacted the hydrogen production in the sequence reaction temperature>methane partial pressure>steam partial pressure. The sensitivity analysis might assist identify how resources should be spent.

- **Keywords:** Artificial neural networks; Process intensification; Steam methane reforming; Hydrogen; Nonlinear response surface techniques

Mingyuan Gu, Yiwei Zhong, Lijun Wang, Zhancheng Guo. *Separation of heavy metals from hazardous lead slag by carbothermic reduction and thermal volatilization: Effect of phase transformation on Sn, Pb, Zn removal*. Pages 330-339.

In this study, the carbothermic reduction and volatilization were applied to recover valuable metals from lead slag. The removal and volatilization mechanisms, especially the migration and distribution behavior of heavy metals, were investigated. The results showed that the removal ratio of Sn was lower than those of Pb and Zn. Increasing the temperature was beneficial to the removal of Zn, but unfavorable for the removal of Sn and Pb. SEM/EDS analysis of the reduced pellets and the flue dust showed that ZnFe2O4 and ZnS in the raw slag were reduced to Zn for volatilization and then reoxidized and formed ZnO(s) in the flue. At lower temperatures, SnO2 and FeOx·PbO·SiO2 in the raw slag was reduced to the volatile SnO and PbO. However, SnO and PbO were further reduced to nonvolatile metallic Sn and Pb at higher temperatures. Fe-Sn and Fe-Pb alloys easily formed when metallic Sn and Pb coexisted with metallic Fe, leading to lower removal ratios. For the metallization of Fe, the iron grains grew up gradually and easily formed joined crystals at higher temperatures, which inhibited the volatilization of Sn and Pb.

- **Keywords:** Lead slag; Carbothermic reduction; Heavy metal removal; Metallized pellet; Comprehensive utilization

Xiaofeng Li, Guohua Chen, Kongxing Huang, Tao Zeng, Xinyu Zhang, Peng Yang, Mulin Xie. *Consequence modeling and domino effects analysis of synergistic effect for pool fires based on computational fluid dynamic*. Pages 340-360.

Synergistic effects of pool fires in fire-induced domino accidents can result in greater damage than single pool fire. Existing research mainly adopts a superposition method based on simplified assumptions to analyze the contribution of synergistic effect of pool fires for domino effects. Therefore, the synergistic effect of pool fires has not been well understood. In this study, a new CFD-based method is developed to model the synergistic effect of pool fires. Case studies were carried out taking double pool fires as an example. The influence of key factors, including wind speed, vertical fire location, fuel type, and separation distance has been investigated quantitatively. The results demonstrated that the proposed CFD based approach can model the consequences of pool fires more comprehensively and assess the domino effects under synergistic effect more precisely than the traditional superposition method. Compared with the single pool fire, the synergistic effect of double pool fires can increase the probability of domino accidents for the adjacent tanks at the downwind by six orders of magnitude. In addition, it is observed that the received maximum radiation heat flux and escalation probability of the target tank in the downwind direction rise with increased wind speed. While the maximum radiation heat flux received by target tanks and escalation probability reduced with increased separation distance and vertical fire location. Moreover, according to the minimum safety distance recommended by present design standards, the synergistic effect of double pool fires in diesel storage tank farms will lead to a higher escalation probability of near equipment than gasoline storage tank farms. This study can be used to predict accident consequences and assess the domino effect under the synergistic effect of pool fires, and guide the layout optimization of the chemical storage tank area.

- **Keywords:** Synergistic effect; Pool fires; CFD; Consequence modeling; Domino effect; Radiation heat flux

Ao Fan, Hongjian Gao. *Synthesis of MgO nanostructures through simple hydrogen peroxide treatment for carbon capture*. Pages 361-372.

The acceleration of global warming induced by uncontrolled CO2 emission has placed a potential threat to human survival and development. The unique properties of magnesium oxide (MgO) including having appropriate surface basicity, low regeneration temperature and high theoretical CO2 uptake capacity make it a promising adsorbent candidate for CO2 capture. Herein, the development and investigation of structure-activity relationships of MgO nanostructures prepared via simple hydrothermal-calcination synthesis method for CO2 capture were reported in this work. The correlation of structural characteristics and basic site properties of MgO samples were discussed by implementing a variety of analytical technologies including BET, SEM, XRD, TPD, Malvern Mastersizer and XPS. The TPD, XPS analysis as well as Claisen-Schmidt condensation reaction show that the hydrothermal-calcination process strongly reduced crystal size and transformed high, low, and moderate basic sites at different ratios for MgO samples. Particularly, MgO nanostructures with morphology of irregular tiny nanocrystals (down to ~5 nm) prepared from simple hydrogen peroxide (H2O2) treatment on commercial MgO exposed abundant moderate and strong basic sites demonstrated significantly better performance (1.04–1.73 mmol/g in a wide temperature range of 100–300 oC) than commercial MgO for CO2 capture. Recyclability of prepared MgO absorbents was also examined and a simple H2O2 regeneration method was explored. The proper correlation of structural characteristics and basic site properties of MgO samples vs their CO2 capture performance were established.

- **Keywords:** Magnesium oxide; CO2 capture; Structure-activity relationships; Lewis basic sites

Noura Najid, Soukaina Fellaou, Sanaa Kouzbour, Bouchaib Gourich, Alejandro Ruiz-García. *Energy and environmental issues of seawater reverse osmosis desalination considering boron rejection: A comprehensive review and a case study of exergy analysis*. Pages 373-390.

Recently, the rapid worldwide growth of seawater reverse osmosis (SWRO) desalination capacity has reignited the boron removal challenge in drinking water. The objective of this review is to discuss the recent advances and patents in boron mitigation strategies in SWRO systems, and to present the energy and environmental concerns of SWRO desalination system with boron rejection. First, the operating parameters of SWRO systems that affect boron removal are presented, before we discuss the reported findings and patents of boron control improvement from the standpoint of membrane materials advancement and from the development of various configurations, such as double pass reverse osmosis and hybrid SWRO processes with other separation technologies like ion exchange (IX), nanofiltration (NF), and electrodeionization (EDI). Thereafter, issues over SWRO desalination's detrimental environmental impact are reviewed: thus, seawater intake, brine discharge, and energy consumption constitute the main weaknesses. Then, sustainable solutions are proposed to reduce the environmental burdens. As SWRO desalination is an energy intensive process, exergy analysis emerges as a key tool to assess the performance of this process. Therefore, the use of exergy analysis to SWRO desalination in general and, as an example, to a full-scale SWRO desalination plant located in Spain, are discussed. The findings indicate that the SWRO unit is responsible for over 64% of exergy destruction due to the irreversibilities associated with the large pressure drop and the high salinity of the brine.

- **Keywords:** Seawater desalination; Reverse osmosis; Boron removal; Life cycle assessment; Exergy analysis

Mingjun Li, Feng Zheng, Yongli Xiao, Yunze Guan, Jiao Wang, Qiang Zhen, Yi Yu. *Utilization of residual heat to prepare high performance foamed glass-ceramic from blast furnace slag and its reinforce mechanism*. Pages 391-404.

The world's steel production has been closer to two billion tons per year and the blast furnace slag (BFS) is the maximum solid waste during the iron-smelting and steel-making process. To conserve energy and reduce emissions, on-site treatment of BFS to produce high value-added products has become a trend. In this study, the foamed glass-ceramic (FGC) is prepared by using BFS and waste glass as the base materials and the residual heat of pre-heated furnace as the heat source to simulate the high temperature industrial waste heat. The optimal FGC shows a low apparent density of 0.67 ± 0.052 g cm−3, a high porosity of 61.49 ± 1.90%, a good compressive strength of 3.18 ± 0.11 MPa, an excellent strength-to-density ratio of 4.75 MPa cm3 g−1 and a relatively small water absorption ratio of 7.05 ± 0.95%, which could completely satisfy the application requirements in the field of building construction. Combined with the SEM, XRD and TEM results, it can be found that the new formed CaSiO3 crystals plays a bridging role between the glass phase and the ceramic phase pre-existed in the BFS, which could effectively reinforce the compressive strength. This study provides a simple and feasible route to treat solid waste by using industrial waste heat and offers a new idea to solve the similar resources, energy and environmental issues.

- **Keywords:** Foamed glass-ceramic; Blast furnace slag; Waste glass; Residual heat; Rapid sintering; Reinforce mechanism

Lin Li, Botao Qin, Jishan Liu, Yee-Kwong Leong, Wai Li, Jie Zeng, Dong Ma, Hui Zhuo. *Influence of airflow movement on methane migration in coal mine goafs with spontaneous coal combustion*. Pages 405-416.

Spontaneous coal combustion was proved to cause methane accumulation and methane explosions in coal mine goafs. To avoid possible methane explosions, the empirical engineering measure, ventilation dilution, is proposed in coal mines though its disaster prevention mechanism has not been well understood. Through experimental and numerical simulations, the superposition effect of the air leakage and coal combustion-induced chimney effect was studied to reveal disaster prevention effect of ventilation dilution. Research results show that the high temperature area of coal combustion is steady and can provide continuous buoyancy force to form upward airflow even under ventilation dilution; the drifting methane accumulation is observed under the superposition effect of air leakage and upward airflow; ventilation dilution can weaken and even eliminate methane accumulation by overcoming chimney effect, but an increase in coal combustion temperature will enhance the upward airflow of chimney effect to cause methane accumulation again. The competitive relationship between the coal combustion-induced chimney effect and air leakage provides a new insight to study methane migration for the disaster formation and prevention mechanism.

- **Keywords:** porous chimney effect; airflow competition; methane accumulation; air leakage; ventilation dilution

Xiaobo Cui, Guohui Song, Ailin Yao, Hongyan Wang, Liang Wang, Jun Xiao. *Technical and Economic Assessments of a novel biomass-to-synthetic natural gas (SNG) process integrating O2-enriched air gasification*. Pages 417-428.

To develop a solution for clean gas supply and biomass utilization and indirect renewable power storage, this work proposes a novel SNG process integrating O2-enriched air gasification with O2 purity range of 80–96%. Low-cost vacuum pressure swing adsorption (VPSA) is integrated to produce O2 with purities of 80% and 90%; while cryogenic air separation (CAS) is applied for 96% O2 purity. Besides SNG, the syngas of the methanation product without CO2 separation (SG) is considered as a new type of safe fuel for rural areas. The technical and economic assessments are successively performed based on simulation data. The effects of important operating variables on technical performances are investigated to determine the optimal values. The overall energy and exergy efficiencies of SG reach 68.37% and 62.59%, respectively, while those of SNG achieve 65.69% and 60.38%, respectively. The equivalent unit product costs of SG and SNG are 1.661 ¥/Nm3 and 2.031 ¥/Nm3 at base scenario, respectively, which are quite profitable. The sensitivity analysis of the cost indicates that the products has strong cost competitiveness within the actual fluctuations, and the constraints for SG is much looser than that for SNG to gain profit. The process integrating VPSA has obvious advantages in efficiencies and unit production cost, which come with the price of visible disadvantages in CH4 concentration and higher heating value (HHV). The work is a representative reference for the countries lacking natural gas and valuable to guide the development of O2-enrich air gasifier, process optimization and indirect renewable power storage.

- **Keywords:** O2-enriched air; VSPA; Renewable power; CO2 separation; SNG; Unit production cost

Jia Tian, Yufeng Wang, Xingfei Zhang, Wei Sun, Haisheng Han, Zhiyuan Yu, Tong Yue. *A novel scheme for safe disposal and resource utilization of arsenic-alkali slag*. Pages 429-437.

As solid waste posing a great threat to the environmental system, the disposal of arsenic-alkali slag has become the top priority in the development of the antimony industry. In this paper, a novel technological scheme combining the advantages of chemical precipitation and fractional crystallization is proposed for the safe disposal and resource utilization of arsenic-alkali slag. The scheme is mainly composed of three parts, namely, leaching of arsenic-alkali slag, selective removal of arsenic in the arsenic-alkali solution, and evaporation crystallization of alkali solution. In the leaching part, the optimum leaching parameters are determined by orthogonal tests. In the arsenic and alkali separation part, based on thermodynamic analysis, the selective removal of arsenic from arsenic-alkali solution is realized by forming ammonium magnesium arsenate ($MgNH_4AsO_4$) precipitation. In the evaporation crystallization part, the crystalline product with sodium carbonate (Na_2CO_3) content of 89.87% is obtained by the evaporation crystallization experiment. The whole process does not produce secondary pollution and realizes the reuse of wastewater. The final products are leaching residue, arsenic slag, and sodium carbonate with an arsenic content of 0.83%, 24.93%, and 0.18%, respectively.

- **Keywords:** Arsenic-alkali slag; $MgNH_4AsO_4$; Separation; Recovery

Farayi Musharavati, Shoaib Khanmohammadi, Rasikh Tariq. *Comparative exergy, multi-objective optimization, and extended environmental assessment of geothermal combined power and refrigeration systems*. Pages 438-456.

In the present work a comparative exergy analysis, multi-objective optimization, as well as extended environmental analysis of a geothermal-based power and refrigeration system, is carried out. Different arrangements with the ammonia-water refrigeration cycle, organic Rankine cycle (ORC), and thermoelectric generator (TEG) are investigated. The current work novelties are the presentation of a novel power-refrigeration system driven by a geothermal source and the employment of TEG units to recover geothermal energy, besides extended environmental assessment. The results of sensitivity analysis indicate that the highest net output work capacity is for the suggested system (configuration 3). Exergy analysis exhibits that in all cases, the absorber has the highest exergy destruction rate and one of the lowest exergy efficiency because it is the first component, which gains the heat from the geothermal source. The suggested system produces 495.2 kW net output power and the highest energy efficiency of 19.42%, which are 131.7 kW, and 3.84% higher than configuration 1(base system). Optimization results represent that in the optimum point, $\dot{W}_{net}$ shows about 33.3% improvement compared with the un-optimized condition. It is found that configuration 3 which consists of cogeneration with two loops of ammonia-water power cycle with refrigeration system along with an additional thermoelectric generator for enhanced waste heat recovery has the highest environmental footprints because of multiple components installed that would occupy more space, electricity, materials, and other resources for its construction, operation, maintenance, and end-of-life.

- **Keywords:** Exergy analysis; Genetic algorithm; Geothermal plant; Optimization; Environmental analysis

Mayandi Jeyaraj, Raji Atchudan, Sakthivel Pitchaimuthu, Thomas Nesakumar Jebakumar Immanuel Edison, Palanichamy Sennu. *Photocatalytic degradation of persistent brilliant green dye in water using CeO2/ZnO nanospheres*. Pages 457-464.

In the present work, ceria/zinc oxide (CeO_2/ZnO) nanocomposite has been synthesized by controlled annealing of cerium and zinc precursors. The obtained CeO_2/ZnO nanocomposite was characterized using common analytical methods such as Fourier

transform infrared spectroscopy (FT-IR), UV-Visible diffuse reflectance spectroscopy (UV-DRS), X-ray diffraction (XRD), X-ray photoelectron spectroscopy (XPS) and scanning electron microscopy with energy dispersive spectrum (SEM with EDS) and elemental mapping measurements. The band gap energy of CeO2/ZnO nanocomposite was about ~2.9 eV calculated from the Tauc plot. The XRD pattern of CeO2/ZnO nanocomposite consisted mixed phases of CeO2 and ZnO with crystalline nature. The XPS spectrum of CeO2/ZnO revealed the presence of C, Zn, N, O and Ce elements, where Zn and Ce existed in 2+ and 4+ oxidation states, respectively. The particle size and shape of synthesized CeO2/ZnO nanocomposite was approximately 0.32 μm with a distorted spherical shape identified from the SEM images. The synthesized CeO2/ZnO nanocomposite effectively degraded BG in water and the calculated kinetic rate constant was 0.0471 min−1. The results suggested that CeO2/ZnO nanocomposite behave as a good photocatalyst towards the degradation of BG, identified from the quick degradation as compared with pure ZnO and CeO2. The enhanced catalytic performance of CeO2/ZnO nanocomposite was attributed to the synergistic effect of both CeO2 and ZnO semiconductors, which decrease the bandgap energy and increase the degradation kinetics.

- **Keywords:** Photocatalyst; CeO2/ZnO nanocomposite; Brilliant green; Decolorization; Synergistic effect

Huizhou Liu, Jinqiu Hu. *An adaptive defect detection method for LNG storage tank insulation layer based on visual saliency*. Pages 465-481.

As the core equipment of the industrial chain, the LNG storage tank is developing in the direction of large-scale and increasing attention has been paid to its economy and safety. The defects of the insulation layer not only affect the insulation performance of the tank but also easily induce safety accidents. To automatically detect these defects, considering the large temperature difference between the defect area and other areas, an adaptive detection method based on infrared thermal imaging technology and a saliency detection algorithm is proposed. Firstly, the median filtering and the Contrast Limited Adaptive Histogram (CLAHE) are introduced to reduce noise and smooth the image. Then, the Adaptive Simple Linear Iterative Clustering algorithm (A-SLIC) based on the entropy of the image is purposed for super-pixel segmentation. After super-pixel segmentation, the saliency map is obtained by manifold ranking, and the salient areas that contain defects of the insulation layer will be segmented automatically. The proposed method is compared with other traditional algorithms on the MSRA1000 dataset and the infrared thermal imaging dataset of LNG storage tanks. The results of the experiments illustrate the effectiveness of the method proposed.

- **Keywords:** Visual saliency; Infrared thermal imaging; Insulation layer defects; Adaptive detection

Yue Han, Xingwei Zhen, Yi Huang. *Hybrid dynamic risk modelling for safety critical equipment on offshore installations*. Pages 482-495.

Safety-critical equipment (SCE) are important safety barriers installed on offshore installations to prevent the occurrence as well as mitigate the consequence of major accidents. Risk assessment is significant for SCE in consideration that the risk of major accidents is increased due to the harsh operational environment and the hazards introduced by periodical preventive maintenance (PM). However, it is difficult to access risk precisely or robustly as the dynamic characteristics of SCE degradation and the influence of human error can increase the uncertainties. In view of this, this study proposes a new hybrid dynamic risk modelling methodology for SCE on offshore installations to capture the causality and dynamic dependencies precisely, where dynamic Bayesian network (DBN) technique and support vector regression (SVR) algorithm are combined. The impact of human error is evaluated through a complex structure

modelling of risk influence factors (RIFs) in DBN. The hybrid SVR-DBN methodology is applied in the case study to assess the dynamic risk profile of a typical SCE (pressure safety valve, PSV) in the context of operation and maintenance respectively. The effectiveness of the hybrid SVR-DBN methodology is verified and the synergy from the integration of SVR and DBN overcomes the limitations of traditional DBN for modelling actual dynamic dependency between dynamic nodes in jacent time-slices. Besides, the modelling of RIFs introduced in DBN facilitates the assessment of human error. The hybrid SVR-DBN methodology is a systematic tool for the dynamic risk assessment of SCE on offshore installations in consideration of both the dynamic characteristics of SCE degradation and the influence of human error.

- **Keywords:** Dynamic risk assessment; Maintenance-related risk; Offshore safety critical equipment; Dynamic Bayesian network; Support vector regression

N.S. Hassan, A.A. Jalil, M.S. Azami, A.F.A. Rahman, M.L. Firmansyah, W. Nabgan. *Photodegradation of bisphenol A from aqueous solution over reduced graphene oxide supported on tetragonal silica-zirconia nanocatalysts: Optimization using RSM*. Pages 496-507.

Bisphenol A (BPA) is an endocrine disruptor, and removing it from contaminated water is a major environmental concern. Herein, graphene derivatives such as graphene (G), graphene oxide (GO), and reduced graphene oxide (rGO) supported silica-zirconia (SZ) were successfully synthesized for photodegradation of BPA. The photodegradation of BPA was ordered as follows: rGO/SZ (88%)>GO/SZ (63%)>G/SZ (58%)>SZ (55%). This is because rGO has bigger regions for π-π stacking and less negatively charged carboxyl groups, which BPA has a higher adsorption affinity than GO. In addition, the highest degradation is predominantly due to the high number of carbon-support interactions and defects sites, including oxygen vacancy. This encouraged effective mobility of charge carriers and subsequently enhanced photoactivity. In this study, the rGO/SZ catalyst was chosen to optimize further the reaction parameters including catalyst dosage, pH and initial concentration of BPA. According to the analysis of variance, the catalyst dosage was the most important variable in the degradation of BPA, followed by pH and initial concentration. The optimum BPA degradation predicted from response surface methodology is 88% at conditions of 8.09 mg L−1 using 0.469 g L−1 of rGO/SZ at pH 6.1, which is reasonably close to the predicted value (89.8%). The rGO/SZ catalyst was found to be stable even after five cycles in the reusability testing.

- **Keywords:** Optimization; RSM; Bisphenol A; Reduced graphene oxide; Silica-zirconia

Mohammed Aatif Shahab, Mohd Umair Iqbal, Babji Srinivasan, Rajagopalan Srinivasan. *Metrics for objectively assessing operator training using eye gaze patterns*. Pages 508-520.

Process plant operators rely on their knowledge of process cause-and-effect relationships during abnormal situation management. Novice operators develop such process knowledge during training. Hence, holistic assessment of operators' training is essential to ensure process safety. Currently, during training, operators' process understanding is evaluated using criteria such as successful completion, task based measures, and operator actions that ignore their cognitive behavior. In this work, we propose an eye-tracking-based approach that uses the operator's attention allocation during different pre-specified training scenarios along with process data, alarm information, and operator actions. Our approach is based on the precept that an operator would focus their attention on those variables on the human-machine interface that they believe have a direct causal relationship to the situation at hand. Also, expert operators seek time-based information for proactive monitoring. Accordingly, to quantify the progress of a novice

operator's learning, we develop two metrics — association metric and salience metric — using correspondence analysis of operators' eye gaze. To evaluate the applicability of the metrics, we conducted experiments with ten participants who performed 486 tasks. Statistical studies reveal that the proposed metrics can quantify operators' learning and thus can be used to objectively evaluate training effectiveness.

- **Keywords:** Operator training; Eye-tracking; HMI; Correspondence analysis; Learning; Attention

Liyang Li, Xu Zhai, Juncai Wang, Peng Chen, Congling Shi. *Experimental study on vertical spill fire characteristics of transformer oil under continuous spill condition*. Pages 521-530.

A vertical spill fire is one of the typical phenomena in fire scenes, which usually occurs with liquid fuel usage and storage and may pose a threat to process safety. In this study, a number of transformer oil continuous spill fire experiments were carried out on a steel experimental setup, in order to obtain the vertical spill fire characteristics of transformer oil or fuels that have similar properties as transformer oil. The flame shape, temperature and radiation data in the process of flame propagation were recorded. According to the change of the burning area, the formation and development process of a vertical spill fire can be divided into four stages. The relationship between burning area and fuel leakage rate in the quasi-stable combustion stage is analyzed and a prediction model for the burning area of a transformer oil vertical spill fire is established. The radiation model of a transformer oil vertical spill fire is established as a function of leakage rate. Based on heat transfer analysis, a mass burning rate model is derived and verified by experimental data.

- **Keywords:** Spill fire; Transformer oil; Vertical plane; Flame spread

Ke GAO, Shengnan LI, Bin SU, Yujiao LIU, Xiaoqi WANG, Lianzeng SHI. *Hole/pore-scale investigation of gas explosions in a coal-mine gob*. Pages 531-544.

The characteristics of a gas explosion were investigated with regard to the hole/pore scale in a coal-mine gob. A 3-D hole-pore single-layer network model (3-D HPSLNM) was developed, and the effects of the length-to-diameter ratio (L/D), ignition location, and gas concentration on the explosion flame and overpressure were determined with the FLACS flame acceleration simulator (Gexcon). The flame propagation speed was positively correlated with L/D and was lower in the hole than in the pores. The overpressure increased linearly with L/D. The flame propagation shape stretched and developed in different ways depending on the ignition location. The maximum flame speed and maximum overpressure for 'end ignition' were 56.5% and 25.2% higher than for 'edge ignition', respectively. The findings of this study will help further research into the hole/pore-scale effects of gas explosions in coal-mine gobs.

- **Keywords:** Gas explosion; Gob; Coal mine; 3-D hole-pore single-layer network mode

Ying Li, Yawei Wang, W.P. Fan, Yan HUO, Conglin Liu, Y. Gao. *Experiment and simulation of JP-5 vapor/air mixture deflagration in enclosed space*. Pages 545-558.

To evaluate the deflagration risk of a premixed gas containing air and high-flash-point JP-5 jet fuel vapor, deflagration experiments were conducted in 1-m^3 and 8-m^3 closed vessels. The variations in deflagration pressure, flame propagation velocity, temperature, and other parameters under different concentrations and vessel volumes were studied. A

large eddy simulation with a premixed gas combustion model was performed, and the obtained results were validated based on full-scale experimental data. The influence of the baffle-blocking ratio on the deflagration hazard was studied. The experimental results highlight the variation trend and numerical range of the deflagration pressure and flame propagation velocity of JP-5 vapor/air mixtures in a closed vessel. An increase in the deflagration vessel volume only extended the pressure rise time and reduced the rate of pressure change. The numerical simulation results supplemented and explained the experimental flame propagation and pressure variation and provided a more realistic deflagration temperature. The baffles in the closed vessel increased the flame turbulence and the rate of pressure rise and enhanced the deflagration hazard.

- **Keywords:** High-flash-point jet fuel; Deflagration in enclosed space; JP-5 vapor/air mixture; Large eddy simulation

Aleinnys M.Barredo Yera, Pérola C. Vasconcellos. *Pesticides in the atmosphere of urban sites with different characteristics*. Pages 559-567.

São Paulo, Brazil, is the greatest pesticide consumer, and associated health problems in local population have already been described. PM2.5 samples were collected in three sites with distinct characteristics and ten pesticides were determined. Population inhalation risk and influence of atmospheric transport in pesticide concentration were evaluated. In the agricultural site, the compounds with higher frequency of detection and concentrations were λ-cyhalothrin, kresoxim-methyl, and atrazine, while in urban and industrial sites, permethrin and malathion. Backward trajectories showed the influence of atmospheric transport. The highest values of daily inhalation exposure in infants were for heptachlor in all three sites. Values of hazard quotients indicated that there is no danger for the exposed population. On the other hand, cancer risk potential results were higher than values recommended by EPA to heptachlor and malathion.

- **Keywords:** Pesticides concentration; Air pollution; Atmospheric transport; Risk assessment

Xiaolei Wang, Yuanping Cheng, Dongming Zhang, Han Yang, Xiao Zhou, Zhigang Jiang. *Experimental study on methane adsorption and time-dependent dynamic diffusion coefficient of intact and tectonic coals: Implications for CO2-enhanced coalbed methane projects*. Pages 568-580.

CO2-enhanced coalbed methane (CO2-ECBM) technology can be applied not only to extract coal seam gas, but also to geologically store a large amount of CO2 produced in various industries, thus reducing the CO2 concentration in the atmosphere and protecting the earth's environment from the adverse effects of climate change. For CO2 injection and methane recovery from coal seams, the differences in the gas adsorption and diffusion characteristics due to the properties of the coal seam are crucial. In this study, first, intact and tectonic coals were collected to conduct a proximate analysis and high-pressure methane adsorption/desorption tests. Subsequently, the adsorption characteristics of the intact and tectonic coals with different particle sizes were analyzed. A time-dependent dynamic diffusion coefficient was introduced to investigate the diffusion characteristics of the two coals. The results showed that the intact and tectonic coals have higher adsorption capacity for CO2 than methane under the same particle size, demonstrating the potential for storing a large amount of CO2 in coal seams. The time-dependent dynamic diffusion coefficient decreased significantly in the initial stages and then tended to stabilize as the desorption progressed. To better explain the gas diffusion characteristics of the coal, a gas diffusion mechanism model was established to analyze the variation in the diffusion coefficient over time. In addition, a new method for reducing the pressure difference was proposed to maximize CO2 storage and methane

recovery. Finally, the environmental implications and safety of CO2 storage in coal seams during the implementation of a CO2-ECBM project was analyzed.

- **Keywords:** Intact and tectonic coals; Methane adsorption; Diffusion; Greenhouse gas control; CO2-ECBM

Xiaotian Bi, Jinsong Zhao. *A novel orthogonal self-attentive variational autoencoder method for interpretable chemical process fault detection and identification*. Pages 581-597.

Industrial processes are becoming increasingly large and complex, thus introducing potential safety risks and requiring an effective approach to maintain safe production. Intelligent process monitoring is critical to prevent losses and avoid casualties in modern industry. As the digitalization of process industry deepens, data-driven methods offer an exciting avenue to address the demands for monitoring complex systems. Nevertheless, many of these methods still suffer from low accuracy and slow response. Besides, most black-box models based on deep learning can only predict the existence of faults, but cannot provide further interpretable analysis, which greatly confines their usage in decision-critical scenarios. In this paper, we propose a novel orthogonal self-attentive variational autoencoder (OSAVA) model for process monitoring, consisting of two components, orthogonal attention (OA) and variational self-attentive autoencoder (VSAE). Specifically, OA is utilized to extract the correlations between different variables and the temporal dependency among different timesteps; VSAE is trained to detect faults through a reconstruction-based method, which employs self-attention mechanisms to comprehensively consider information from all timesteps and enhance detection performance. By jointly leveraging these two models, the OSAVA model can effectively perform fault detection and identification tasks simultaneously and deliver interpretable results. Finally, extensive evaluation on the Tennessee Eastman process (TEP) demonstrates that the proposed OSAVA-based fault detection and identification method shows promising fault detection rate as well as low detection delay and can provide interpretable identification of the abnormal variables, compared with representative statistical methods and state-of-the-art deep learning methods.

- **Keywords:** Process monitoring; Orthogonal attention; Variational self-attentive autoencoder; Fault detection; Fault identification

Xingyuan Gao, Jinyu Li, Mudi Zheng, Shiyi Cai, Jieyi Zhang, Saeed Askari, Nikita Dewangan, Jangam Ashok, Sibudjing Kawi. *Recent progress in anti-coking Ni catalysts for thermo-catalytic conversion of greenhouse gases*. Pages 598-616.

As global warming has become a major environmental problem, how to effectively reduce or rationally utilize greenhouse gases has become an important topic. This review summarizes the latest development of Ni-based catalysts for thermal-catalytic conversion of CO2 and CH4, including steam reforming of methane, partial oxidation of methane, methane decomposition, dry reforming of methane, reverse water gas shift reaction and CO2 hydrogenation. The modification strategies are illustrated in depth, such as size and dispersion control, surface modification, oxygen defects. Besides, the reaction and coking mechanisms for various processes are introduced, and the effects of reaction conditions and reactor designs are discussed and illustrated. This is the first comprehensive review on discussing the latest developments of anti-coking Ni-based catalysts for six commonly studied thermal-catalytic processes where two greenhouse gases (CH4 and CO2) are involved. To further improve the catalytic performances and energy efficiency, advanced techniques such as plasma and microwave can be integrated and in-situ characterizations are expected to explore the deactivation mechanisms in depth. Moreover, a smart design

of the catalyst is necessary to inhibit the side reactions by changing the reaction pathways.

- **Keywords:** Thermo-catalytic reaction; CO2; CH4; Ni catalysts; Carbon deposition; Greenhouse gas

Younjeong Choe, Junho Lee, Woosang Jung, Jonghak Park, Jungho Lee, Jae Young Jho, Kyu Tae Lee, Taewoo Kim, Yong Hyup Kim. *Gravity-based oil spill remediation using reduced graphene oxide/LDPE sheet for both light and heavy oils*. Pages 617-624.

Oil spill is a catastrophic accident to environment and human beings, requiring a rapid response to reduce the damage. The conventional oil collecting techniques based on adsorption or filtration, however, are not suitable for rapid response because of their performance dependence on oil types. Here we show that an oil collection technique based on gravity, unlike the conventional schemes based on adsorption or filtration, enables collection of light as well as heavy oils regardless of the viscosity. A solid sheet, which is lighter than water but heavier than oil, would be placed by gravity between oil and water, thereby physically separating oil from water. This fact is utilized to devise a simple and yet efficient oil recovery scheme. The oil on the sheet, over 10 cm in diameter and 0.18 mm in thickness, is drawn into a reservoir by gravity through a 4 mm tube connected to a hole in the center of the sheet. The sheet floating on water can recover oil at a rate of ~1,150,000 L m−2 h−1 that is an order of magnitude higher than that obtainable from filtration methods. We expect this nature-provided oil recovery scheme, which is autonomous, inexpensive, and fast, would provide a quick oil spill remediation regardless of the oil type, thereby minimizing the damage to environment and human beings.

- **Keywords:** Oil separation; Density difference; Gravity; Reduced graphene oxid